Journal of Nuclear Materials 399 (2010) 26–31

Contents lists available at ScienceDirect

Journal of Nuclear Materials

journal homepage: www.elsevier.com/locate/jnucmat

# One-dimensional motion of self-interstitial atom clusters in A533B steel observed using a high-voltage electron microscope

T. Hamaoka [a,*], Y. Satoh [a], H. Matsui [b]

[a] Institute for Materials Research, Tohoku University, 2-1-1 Katahira, Aoba-ku, Sendai 980-8577, Japan
[b] Institute of Advanced Energy, Kyoto University, Gokasho, Uji-shi, Kyoto 611-0011, Japan

ARTICLE INFO

*Article history:*
Received 27 January 2009
Accepted 24 December 2009

ABSTRACT

One-dimensional motion of self-interstitial atom clusters in A533B steel was observed using high-voltage electron microscopy. The frequency and distance of one-dimensional motion under electron irradiation were measured. One-dimensional motion occurred frequently at room temperature, but it occurred only slightly at 563 K. The frequency of one-dimensional motion was decreased by annealing at 473 K and higher temperatures. The decreased motion frequency gradually increased under prolonged irradiation. Although annealing reduced the motion frequency of clusters that had been formed before annealing, reduction of the motion frequency was not detected for clusters that formed after annealing.



## 1. Introduction

Irradiation of high-energy particles introduces self-interstitial atoms (SIAs), vacancies, and their individual clusters into materials. Results of experiments [1–7] and molecular dynamics (MD) simulations [8–13] have demonstrated that SIA clusters move one-dimensionally, conforming to some particular crystallographic orientations. Vacancy-type clusters also perform one-dimensional (1D) motion [14,15]. Prior reports have described that the 1D motion of SIA clusters plays an important role in the microstructural evolution of materials under irradiation [9,16–21]. Therefore, it is important to elucidate the mobility of SIA clusters in nuclear reactors under service conditions. Furthermore, it is important to understand the extent to which 1D motion affects microstructural evolution. Investigations of pure metals and binary alloys using a high-voltage electron microscope (HVEM) have revealed that some impurities and alloying elements reduce the 1D motion of SIA clusters [2,4,7]. Moreover, the reduction of 1D motion appears even when solutes are present in very small concentrations [7]. Judging from these findings, one might infer that 1D motion occurs only slightly in commercial materials containing larger amounts of alloying elements.

From in situ observations using HVEM, we examined the 1D motion of SIA clusters in A533B steel, which is used for reactor pressure vessels (RPV) in nuclear power plants. The experimental results are discussed from viewpoints of interactions between SIA clusters and solute atoms.

## 2. Experimental methods

### 2.1. Sample

The A533B steel used for this study was A533B CL1 that had been standardized by the American Society for Testing and Materials. Its nominal composition is presented in Table 1. The composition described in Table 1 is not an assay value. The concentration of interstitial impurities determined by chemical analyses is presented in Table 2. Before chemical analyses, oxide surface layers of the sample had been removed by chemical polishing in a solution of 3 ml of 46% hydrogen fluoride acid (HF), 50 ml of 30% hydrogen peroxide ($H_2O_2$), and 6 ml of distilled water ($H_2O$). After polishing, the sample was rinsed in a solution of 40 ml of 30% $H_2O_2$ and 40 ml of $H_2O$; then it was washed in $H_2O$, and subsequently, in ethyl alcohol ($C_2H_5OH$).

Preparation of specimens for in situ observations using an HVEM proceeded as follows. A sheet of A533B steel more than 0.6 mm thick was cut very slowly from the block using a low-speed saw. The sheet was chemically polished to about 0.1 mm thickness in a solution of HF, $H_2O_2$, and $H_2O$ to remove damaged areas from the surface. Disks of 3 mm diameter were punched out from the sheet. They were then thinned using a twinjet electrolytic polishing method with a solution of 50 ml of 60% perchloric acid ($HClO_4$) and 950 ml of $C_2H_5OH$ at room temperature at a voltage of 80 V. The thinned disks were then electropolished using this solution, which had been cooled by liquid nitrogen at a voltage of 31 V at a current of less than 0.1 A with a stainless cathode. After polishing, the disks were washed in $C_2H_5OH$.

Next we describe a preparation of smaller specimens, which were used to reduce the effect of ferromagnetism of the A533B steel in observations using a conventional transmission electron

* Corresponding author. Tel.: +81 022 215 2069; fax: +81 022 215 2066.
*E-mail address:* hamaoka@criepi.denken.or.jp (T. Hamaoka).

0022-3115/$ - see front matter © 2010 Elsevier B.V. All rights reserved.
doi:10.1016/j.jnucmat.2009.12.014

**Table 1**
Nominal composition of the A533B steel used for this study (wt.%).

| Mn | Mo | Ni | Cu | V | Si | P | S | C | Fe |
|---|---|---|---|---|---|---|---|---|---|
| 1.34 | 0.45 | 0.50 | 0.055 | 0.004 | 0.25 | 0.013 | 0.017 | 0.20 | Balance |

**Table 2**
Concentration of interstitial impurities in the A533B steel determined through chemical analyses.

| C (wt.%) | H (wppm) | N (wppm) | O (wppm) |
|---|---|---|---|
| 0.19 | <1 | 101 | 41 |

microscope (TEM). A sheet of more than 0.6 mm thickness described in the preceding paragraph was chemically polished to less than 0.05 mm thickness. The sheet was electropolished using the method described above (without the twinjet polishing); then it was washed. The thinner part of the sheet was cut off with a knife and sandwiched between meshes made of copper.

### 2.2. In situ observations using an HVEM

Electron irradiation and in situ observations were conducted using JEM-ARM1250 (JEOL) operated at an acceleration voltage of 1250 keV. Irradiation was done at room temperature or 563 K, which is close to the temperature at which A533B steels are used in functioning nuclear reactors. The electron flux was $3 \times 10^{24}$ e m$^{-2}$ s$^{-1}$; which corresponds to a damage rate of $2 \times 10^{-2}$ dpa s$^{-1}$ [22] with 20 eV applied as the displacement threshold energy. Specimens were polycrystalline with small grains and had a large density of dislocations. We observed areas that were well separated from grain boundaries and which had few dislocations. The thickness of observed areas was about 100–150 nm. Suitable grain orientations along 110 Kikuchi lines except for zone axis conditions were selected under irradiation. Bright field images were observed using a diffraction vector **g** equal to 110. Images on the fluorescent screen were recorded using a charge-coupled device camera at 30 frames per second.

### 2.3. Microstructural changes attributable to annealing

After 1250 keV electron irradiation, using a conventional TEM to avoid displacement of atoms, we inspected the microstructural changes attributable to annealing. Smaller specimens described in Section 2.1 were irradiated using HVEM at room temperature for about 500 s (10 dpa) to introduce SIA clusters. One of these specimens was observed with TEM at room temperature at an acceleration voltage of 200 keV. This specimen was annealed at 563 K for 60 min in a vacuum of less than $5 \times 10^{-4}$ Pa in a quartz tube. The irradiated area was observed again at room temperature using TEM. To inspect the microstructural change accurately, both TEM observations before and after annealing were conducted at almost identical orientation. Furthermore, to equalize the inside–outside condition before and after annealing, we used an identical condition for the sign of the diffraction vector 110 and excitation error.

We also conducted in situ observations at 673 K using a heating specimen stage in TEM to investigate the changes of irradiation-induced microstructures during annealing.

## 3. Results

### 3.1. Accumulation process of point defect clusters

Defect clusters with black dot images of about 2 nm appeared after several minutes' irradiation with 1250 keV electrons. The defect clusters grew slowly and their number density increased during successive irradiation. We inspected the defect clusters of 2–8 nm. Large defect clusters showed a clear dislocation loop contrast. We have not identified the nature of the defect clusters. However, it is likely that most clusters were of interstitial type, for reasons which will be described later in Section 4.1. The 1D motion of the clusters certainly occurred under 1250 keV electron irradiation. Observations of 1D motion were conducted under conditions in which new clusters were constantly appearing. The behavior of 1D motion showed no marked dependence on the electron fluence.

### 3.2. Motion frequency

By counting the black dot images and 1D motion in the recorded HVEM images, we determined the motion frequency, which we defined as the average number of 1D motions observed per single SIA cluster during unit time. The rules used to count 1D motion were the following.

- The most often observed 1D motion is that a black dot image, which had been stationary, moves several nanometers during one-thirtieth of a second (1/30 s) and then becomes stationary again. We counted such a movement as one 1D motion.
- Sometimes, defect clusters moved slowly, taking a few seconds to move a few nanometers. We considered the entire event of such a slow movement as one 1D motion.
- The 189-mm-wide and 98-mm-high bright field images on the display of a personal computer were used to count clusters and 1D motion. The images correspond to about 580,000× magnification. A pixel was about 0.9 nm. We were unable to count 1D motions over short distances that were not observable at this magnification.
- Back-and-forth motion of clusters between two positions was observed occasionally. We counted one back-and-forth motion as two 1D motions.
- In the A533B steel, most 1D motions occurred along ⟨1 1 1⟩: the close-packed direction of the atom array. In addition, 1D motions along ⟨1 0 0⟩, the second close-packed direction, were observed occasionally. We can say that at least 95% of all 1D motions of which the moving directions were determined definitely were along ⟨1 1 1⟩. We counted 1D motions, irrespective of their direction. We did not determine the Burgers vectors of SIA clusters in a stationary state. However, it is clear that most Burgers vectors of moving clusters were 1/2⟨1 1 1⟩ because a moving cluster invariably possesses a Burgers vector parallel to the moving direction.
- It is occasionally observed that point defect clusters of several nanometers appear suddenly in the field of view (FOV). Some clusters might have come to the FOV by 1D motion from the outside. Alternatively, the sudden appearance of an SIA cluster might have resulted from coalescence with another SIA cluster, which can cause a change of their Burgers vectors **b** and the sudden appearance by the breakdown of $\mathbf{g} \cdot \mathbf{b} = 0$ condition. Therefore, we counted the sudden appearance as one 1D motion.
- We also counted a sudden disappearance of a defect cluster of the FOV as one 1D motion because the disappearance is attributable to escapes through 1D motion to the outside of the FOV or the surface of specimens.
- 1D motion of SIA clusters near the surface of specimens might have been affected by the image force. However, we did not consider the image force in counting the 1D motion.

#### 3.2.1. Dependence of motion frequency on irradiation time

Fig. 1 presents the motion frequency at room temperature under 1250 keV electron irradiation. Frequencies in four FOVs are

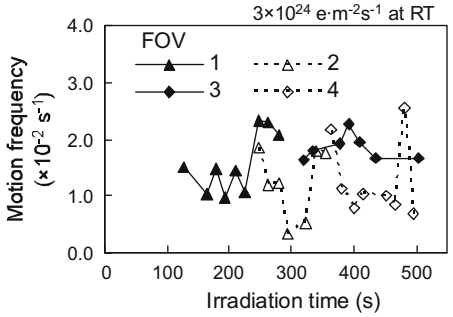


**Fig. 1.** Dependence of the motion frequency at room temperature on irradiation time. The motion frequencies in four fields of view are shown. Each data point represents the average frequency for 15 s.

**Table 3**
Motion frequencies at room temperature and at 563 K under electron irradiation.

| Temperature | Frequency |
|---|---|
| RT | $1.7 \times 10^{-2}\,s^{-1}$ |
| 563 K | $0.1 \times 10^{-2}\,s^{-1}$ |

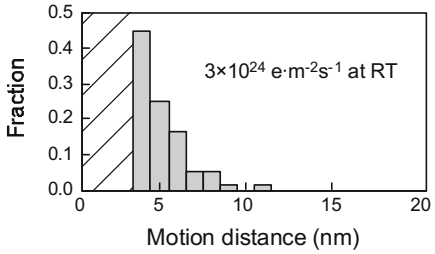


**Fig. 2.** Distribution of 1D motion distances at room temperature under electron irradiation. Distances of 4 nm and more are shown.

portrayed, although frequencies of nine areas were measured in all. Each data point represents the average frequency for 15 s. The abscissa is the irradiation time measured from the start of each HVEM image recording. Before recording, we irradiated each area for several minutes to obtain a preferred orientation of the specimen and diffraction vector. The frequencies fluctuated with irradiation time, but showed no obvious time dependence. This was true for the five areas not presented in Fig. 1.

### 3.2.2. Comparison of motion frequency at room temperature and at 563 K

Table 3 presents a comparison of the motion frequencies at room temperature and 563 K. For the 563 K case, all clusters were introduced at this temperature. Considering that the frequency at room temperature had no apparent time dependence, we expressed it by the average for all irradiation times and in all FOVs. Regarding 563 K, the average for 4 min in one area is shown. The frequency at 563 K was much lower than that at room temperature. Furthermore, in other FOVs at 563 K, 1D motion rarely occurred.

## 3.3. Motion distance

We defined the motion distance as the distance over which an SIA cluster moves in 1/30 s. We measured 1D motions only along ⟨1 1 1⟩, although 1D motions along ⟨0 0 1⟩ were observed occasionally. By considering inclinations of ⟨1 1 1⟩ to the fluorescent screen, distances in HVEM images were converted to those along the ⟨1 1 1⟩.

Fig. 2 portrays the distribution of motion distances at room temperature under electron irradiation. Only motion distances of 4 nm and greater are shown here because shorter distances can not be measured accurately, although we note that 1D motion of a distance of less than 4 nm was often observed. We did not investigate the electron fluence dependence of motion distances quantitatively. However, significant fluence dependence of motion distances was not found.

## 3.4. Effect of post-irradiation annealing on motion frequency

### 3.4.1. Procedures of the experiments

Under electron irradiation, the behavior of atoms in the material is complicated because atoms are dynamically displaced and irradiation-induced defects can diffuse. For that reason, we tried post-irradiation annealing experiments: we investigated the change of motion frequency caused by annealing at a high temperature without irradiation. The procedure was as follows. First, an area was irradiated with 1250 keV electrons at room temperature to introduce SIA clusters. Then the irradiation was stopped. Annealing was conducted at a high temperature for a given time with a heating stage inside HVEM. Then, the area was irradiated and observed again at room temperature. Motion frequencies before and after annealing were compared.

Several minutes were necessary to reach a new temperature. For example, for annealing at 563 K, each increase and decrease of temperature took about 4 min, even in the case of 5 min annealing.

As Fig. 1 shows, some difference exists in motion frequency between FOVs. Therefore, we compared motion frequencies before and after annealing in an identical area for each annealing condition. The 1D motion happens randomly. Therefore, it is better to observe SIA clusters for a longer time to reduce the statistical error in motion frequency. For the frequency before annealing in an FOV, we used the average of all irradiation times, which is plausible because no apparent fluence dependence of motion frequency has been detected.

On the other hand, as described later, the motion frequency decreased by annealing and then increased gradually with fluence. Therefore, the motion frequency immediately after annealing most properly reflects the effect of annealing. For this reason, and because observation for a longer time is necessary to reduce statistical error, we used the average frequency for 90 s from the resumption of irradiation. A slight change of this time period caused no significant difference in results.

### 3.4.2. Annealing at different temperatures for 20 min

Fig. 3 presents the respective changes of the motion frequency by annealing at 373 K, 473 K, 563 K, and 673 K for 20 min. The ordinate in Fig. 3 is the ratio $R$ of the motion frequency after each

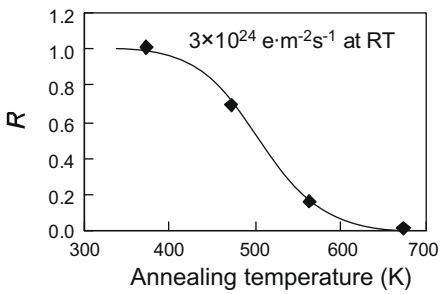


**Fig. 3.** Changes of motion frequency by annealing at 373 K, 473 K, 563 K, or 673 K for 20 min. $R$ is the ratio of the motion frequency after each annealing to the frequency before the corresponding annealing.

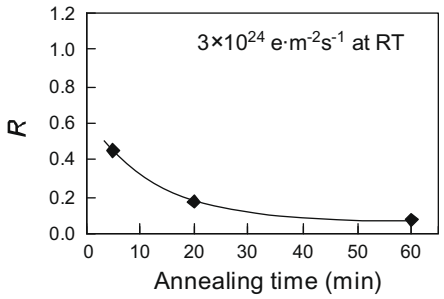


**Fig. 4.** Changes of motion frequency by annealing at 563 K for 5, 20, or 60 min. *R* is the ratio of the motion frequency after each annealing to the frequency before the corresponding annealing.

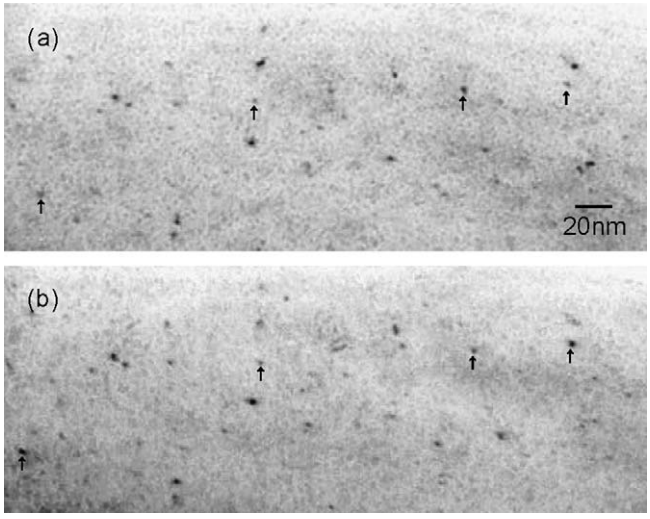


**Fig. 5.** TEM images (a) before annealing and (b) after annealing at 563 K for 60 min. Clear microstructural changes caused by annealing were not detected, although the arrowed SIA clusters moved.

annealing to the frequency before the corresponding annealing. The results show that the frequency was decreased by annealing at 473 K and higher temperatures. The higher the annealing temperature was, the lower *R* became.

In contrast, clusters that were newly produced after annealing in a different area conducted 1D motion as if the annealing had not been done. In other words, the decrease of motion frequency by annealing was not detected on the fresh clusters.

*3.4.3. Dependence of R on annealing time*

Fig. 4 portrays the changes of motion frequency by annealing at 563 K for 5, 20, and 60 min. The motion frequency was reduced by annealing for 5 min. Moreover, *R* decreased concomitantly with increasing annealing time, although the slope in this curve decreased with increasing annealing time.

*3.4.4. Microstructural change caused by annealing*

No clear microstructural change attributable to annealing at 563 K for 60 min was detected, as presented in Fig. 5, although the arrowed clusters in this figure moved during annealing. The maximum distance of the movements was 10 nm. Directions of all movements were ⟨1 1 1⟩. In other words, these clusters, which are probably of interstitial type, made a one-dimensional conservative motion, but did not move by pipe diffusion of the constituent SIAs through the dislocation cores.

Fig. 6 portrays microstructural changes that occurred during annealing at 673 K observed using a heating stage inside 200 keV TEM. Each bottom micrograph is an enlargement of the square region in the corresponding top micrograph. We observed that several clusters shrank and disappeared like a cluster in the circle. Some clusters moved during annealing. One example is the arrow-indicated cluster, which moved 10 nm.

*3.4.5. Prolonged irradiation after annealing*

We conducted prolonged irradiation after annealing and inspected the frequency of 1D motion during irradiation. Fig. 7 portrays quantities of irradiation-induced clusters and 1D motions under irradiation at room temperature in an FOV that had been previously irradiated at room temperature and then annealed at 673 K for 20 min. The number of clusters is expressed as the average for 15 s. The clusters observed after annealing are classifiable into two types: those which had been formed by the irradiation before annealing, and others which appeared during irradiation after annealing. Most of the latter clusters must be those which had been newly formed by the irradiation after annealing. Data points for the two types of clusters are portrayed separately in Fig. 7.

The clusters which had been formed before annealing moved only slightly at the early stage of the irradiation after annealing. However, the prolonged irradiation increased its motion frequency, as emphasized by the broken line in the figure.

The clusters of the other type appeared from about 135 s after the resumption of irradiation, and the number of them in the FOV increased gradually. The motion frequency at the early stage of their appearance was zero. However, this value is statistically meaningless because of the small number of the fresh clusters. Under prolonged irradiation, results showed that they performed 1D motion more often than clusters that had been formed before annealing. Furthermore, it is noteworthy that the motion frequency was close to that before the annealing in the same FOV, $1.8 \times 10^{-2}\ s^{-1}$; that is, no effect of the annealing was detected for the fresh clusters.

## 4. Discussion

### 4.1. Nature of point defect clusters

Point defect clusters having black dot images were formed under 1250 keV electron irradiation. We have not identified the nature of these clusters. However, it is likely that most of these clusters were of interstitial type. Indeed, formation of vacancy clusters under certain irradiation conditions has been demonstrated. For example, Hayashi has described formation of clusters of two kinds, which were clearly distinguishable by their behavior. Hayashi considered one of these clusters to be of vacancy type [23]. On the other hand, in our experiments, all observed clusters behave similarly, which implies that all the observed clusters have the same character, i.e. they are of interstitial type. In addition, vacancy clusters are likely to shrink during successive irradiation by dislocation bias effect. Therefore, it is very probable that most of the clusters observed in this study were of interstitial type and we regard the observed clusters as SIA clusters hereinafter.

As presented in Fig. 6, several clusters shrank and disappeared during annealing at 673 K. It is likely that irradiation-induced vacancies diffused during annealing. These SIA clusters absorbed them to shrink.

### 4.2. 1D motion of SIA clusters in A533B steel

The 1D motion of SIA clusters was observed in A533B steel. The motion behavior under 1250 keV electron irradiation was similar

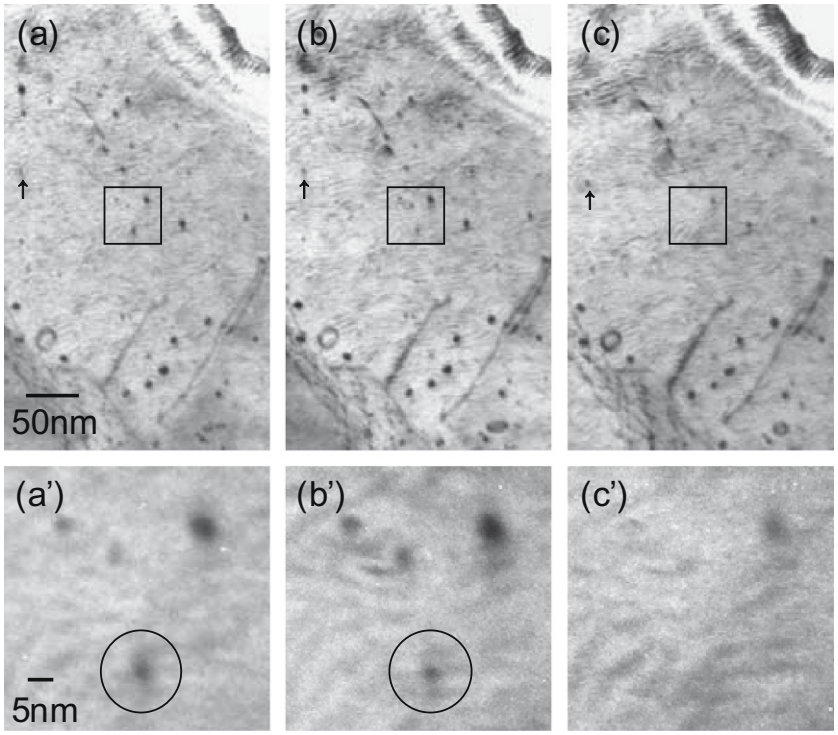


**Fig. 6.** Microstructural change during annealing at 673 K (TEM images). The annealing times are (a and a′) 540 s, (b and b′) 690 s, and (c and c′) 920 s. Each bottom micrograph is an enlargement of the square region of the corresponding top micrograph. We circled a cluster that had gradually shrunk and disappeared. The arrowed cluster moved during annealing.

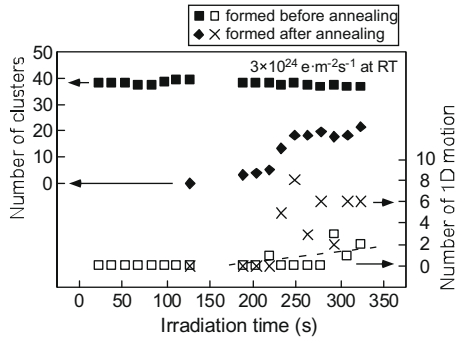


**Fig. 7.** Number of clusters and 1D motions in an FOV under 1250 keV irradiation at room temperature after annealing at 673 K for 20 min. Data points for irradiation-induced clusters of two types – formed before annealing or after annealing – are shown separately. The number of clusters is expressed in the average for 15 s. The number of 1D motions is shown in all counts for each 15 s. The broken line emphasizes the increase of the motion frequency of the clusters that were formed before annealing.

to that in iron and iron-based binary alloys [1,4,7,24], although the motion frequency and motion distance in the A533B steel were lower and shorter than those in the pure materials. Results of this study show that 1D motion of SIA clusters occurs in this engineering steel at the service condition. Results also imply the relation of the 1D motion to microstructural evolutions such as decoration of SIA clusters near dislocations.

Our recent experimental results obtained using high-purity materials [7,24] have been explained with a model in which a single solute atom can pin down an SIA cluster to prevent 1D motion. Actually, A533B steel contains several percent of alloying elements in all. In this alloy, solute atoms are present around the SIA clusters. Accordingly, moving SIA clusters must encounter solute atoms immediately, which leads us to infer the immobilization of SIA clusters. However, the results presented herein have shown that 1D motion actually occurs. The reason why 1D motion can occur in those alloys with high concentration of alloying elements remains unresolved.

As described above, 1D motion occurred only slightly at 563 K even under electron irradiation. In addition, annealing at 473 K and higher temperatures reduced the motion frequency. A mechanism by which the increase of temperature reduces the motion frequency is likely to be segregation of some solute atoms on SIA clusters. Results clarified that in iron–chromium alloys, the solute chromium segregation around SIA clusters retards 1D motion [4]. In A533B steel, segregating solutes are possibly interstitial elements: carbon, nitrogen, and oxygen. It is true the interstitial elements are trapped by irradiation-induced vacancies, but in iron, the binding of a carbon atom and a vacancy can dissociate thermally at 480 K [25], and the binding of a nitrogen atom and a vacancy can dissociate at 473 K [26]. Therefore, the interstitial elements are likely to diffuse rapidly and subsequently segregate around SIA clusters at 473 K and higher temperatures. Three-dimensional atom probe analyses have shown that carbon atoms exist in the form of carbide [27]; accordingly, only solute carbon atoms present the possibility of segregating around SIA clusters. On the other hand, in the presence of radiation-induced point defects, substitutional solute atoms might segregate on SIA clusters. We have not clarified what solutes actually segregated on SIA clusters.

Some clusters moved during annealing (Figs. 5 and 6). It is likely that interstitial element atoms were dragged by the moving clusters as in the case of dynamic strain aging phenomena.

The reduction of motion frequency by annealing has not been detected for SIA clusters that were formed after annealing. This finding suggests that clusters freed from significant segregation of solute atoms can perform frequent 1D motion. Under cascade damage conditions, SIA clusters are formed during about 10 ps

[28,29]. Solute atoms cannot segregate on SIA clusters during such a short period. Therefore, we think that SIA clusters formed directly through cascades have a high probability of performing 1D motion.

The SIA clusters whose motion frequency was decreased by annealing performed 1D motion under prolonged 1250 keV irradiation, as described in Section 3.4.5. This phenomenon is explainable as follows: solute atoms segregating on SIA clusters were resolved by the collision of fast electrons during prolonged irradiation.

## 5. Summary

We conducted in situ observations of 1D motion of SIA clusters in A533B steel under electron irradiation using HVEM. Results revealed that the 1D motion observed in comparatively clean materials certainly occurs also in A533B steel. The present results suggest that the 1D motion can contribute microstructural evolutions in this practical steel under cascade damage conditions. The 1D motion occurred frequently at room temperature, but it occurred only slightly at 563 K. The motion frequency was decreased by annealing at 473 K and higher temperatures. The decrease of motion frequency was not detected on clusters that formed after annealing. These phenomena are explainable using a model in which some solute atoms diffuse rapidly at higher temperatures and segregate on SIA clusters to pin them down.

## Acknowledgements

We thank the staff of the Analytical Research Core for Advanced Materials for chemical analyses. We also thank Messrs. E. Aoyagi and Y. Hayasaka for their technical support in using HVEM. We express our appreciation for the technical support of Mr. S. Ito in using TEM.

## References

[1] M. Kiritani, J. Nucl. Mater. 251 (1997) 237–251.
[2] T. Hayashi, K. Fukumoto, H. Matsui, J. Nucl. Mater. 307–311 (2002) 993–997.
[3] H. Abe, N. Sekimura, Y. Yang, J. Nucl. Mater. 323 (2003) 220–228.
[4] K. Arakawa, M. Hatanaka, H. Mori, K. Ono, J. Nucl. Mater. 329–333 (2004) 1194–1198.
[5] K. Arakawa, M. Hatanaka, E. Kuramoto, K. Ono, H. Mori, Phys. Rev. Lett. 96 (2006) 125506.
[6] K. Arakawa, K. Ono, M. Isshiki, K. Mimura, M. Uchikoshi, H. Mori, Science 318 (2007) 956–959.
[7] Y. Satoh, H. Matsui, T. Hamaoka, Phys. Rev. B 77 (2008) 094135.
[8] B.D. Wirth, G.R. Odette, D. Maroudas, G.E. Lucas, J. Nucl. Mater. 244 (1997) 185–194.
[9] N. Soneda, T. Diaz de la Rubia, Philos. Mag. A 78 (1998) 995–1019.
[10] N. Soneda, T. Diaz de la Rubia, Philos. Mag. A 81 (2001) 331–343.
[11] Yu.N. Osetsky, D.J. Bacon, A. Serra, B.N. Singh, S.I. Golubov, J. Nucl. Mater. 276 (2000) 65–77.
[12] Yu.N. Osetsky, D.J. Bacon, A. Serra, B.N. Singh, S.I. Golubov, Philos. Mag. 83 (2003) 61–91.
[13] J. Marian, B.D. Wirth, A. Caro, B. Sadigh, G.R. Odette, J.M. Perlado, T. Diaz de la Rubia, Phys. Rev. B 64 (2002) 144102.
[14] Yu.N. Osetsky, D.J. Bacon, A. Serra, Philos. Mag. Lett. 79 (1999) 273–282.
[15] Y. Matsukawa, S.J. Zinkle, Science 318 (2007) 959–962.
[16] B.N. Singh, A.J.E. Foreman, Philos. Mag. A 66 (1992) 975–990.
[17] H. Trinkaus, B.N. Singh, A.J.E. Foreman, J. Nucl. Mater. 206 (1993) 200–211.
[18] H. Trinkaus, B.N. Singh, S.I. Golubov, J. Nucl. Mater. 283–287 (2000) 89–98.
[19] T. Yoshiie, Y. Satoh, Q. Xu, J. Nucl. Mater. 329–333 (2004) 81–87.
[20] M. Wen, N.M. Ghoniem, B.N. Singh, Philos. Mag. 85 (2005) 2561–2580.
[21] M.J. Caturla, C.J. Ortiz, J. Nucl. Mater. 362 (2007) 141–145.
[22] O.S. Oen, Cross Section for Atomic Displacement in Solids by Fast Neutrons, ORNL, ORNL-4897.
[23] T. Hayashi, Doctoral Thesis, 2003.
[24] T. Hamaoka, Y. Satoh, H. Matsui, in preparation.
[25] P. Hautojarvi, in: P.G. Coleman, S.C. Sharma, L.M. Diana (Eds.), Positron Annihilation, North-Holland Publishing Company, Amsterdam, 1982, pp. 389–394.
[26] T. Takeyama, H. Takahashi, J. Phys. Soc. Jpn. 38 (1975) 1783.
[27] T. Toyama et al., unpublished results.
[28] T. Diaz de la Rubia, M.W. Guinan, Phys. Rev. Lett. 66 (1991) 2766–2769.
[29] A.J.E. Foreman, W.J. Phythian, C.A. English, Philos. Mag. A 66 (1992) 671–695.